SEARCHES FOR PROMPT HEAVY QUARKONIA & $\mathbf{B_c^{\pm}}$ MESONS AND EVIDENCE FOR RADIALLY EXCITED B MESONS IN $\mathbf{Z^0}$ DECAYS

Gerald Eigen*

Department of Physics, University of Bergen, Allegaten 55
5007 Bergen, Norway

We have searched for prompt heavy quarkonia and B_c mesons in 3×10^6 hadronic Z^0 decays recorded with the DELPHI detector at LEP. No signal was observed in any of these modes. We achieved the highest sensitivities for gluon fragmentation into J/ψ and for semileptonic $B_c^{\pm}$ decays, yielding branching ratio upper limits of $B(Z^0 \to J/\psi ggX) < 4.1 \times 10^{-4}$ and $B(Z^0 \to B_c^{\pm} X) \cdot B(B_c^{\pm} \to J/\psi l^{\pm} \nu_l) < 5.0 \times 10^{-5}$ @ 90% CL, respectively. We found the first evidence for radially excited B mesons, by observing a signal in the $B^{(*)}\pi^+\pi^-$ final state at $Q = m(B^{(*)}\pi^+\pi^-) - m(B^{(*)}) - 2m(\pi) = 301 \pm 4 \pm 10$ MeV.

1. Search for Prompt Heavy Quarkonium Production in Z^0 Decays

Heavy quarkonia are expected to be produced promptly in Z^0 decays. The relevant processes, depicted in lowest order QCD in figure 1, are heavy quark fragmentation, gluon fragmentation and hard gluon radiation. They are suppressed with respect to $Z^0 \to q\bar{q}$ decays, because the gluon squared 4-momentum has to be significantly larger than the QCD scale: $q^2 > 4m_Q^2 >> \Lambda_{QCD}^2$. The suppression contains a factor of $\mid R(0) \mid^2 / m_Q^3$, where $R(0)$ is the nonrelativistic radial wave function at the origin and m_Q is the heavy quark mass.[1,2] Heavy quarkonium production via hard gluon radiation is further suppressed by a factor of m_Q^2/m_Z^2.

Heavy quarkonia can be produced in a color singlet or a color octet. In a pure color singlet model, heavy quark fragmentation is dominant.[3] For J/ψ production the branching fraction obtained from a non-relativistic QCD calculation (NRQCD) is $B(Z^0 \to J/\psi c\bar{c}) = 7.7 \times 10^{-5}$. This includes contributions from the ψ' and the χ_c states. The corresponding branching fractions for gluon fragmentation and hard gluon radiation are reduced by factors of 4 and 200, respectively. For Υ production the branching ratio via b-quark fragmentation is predicted to be $B(Z^0 \to \Upsilon b\bar{b}) = 1.6 \times 10^{-5}$. This is a factor of 8 higher than the prediction for hard gluon radiation.[3] In a color octet model, the gluon fragmenta-

*representing the DELPHI collaboration

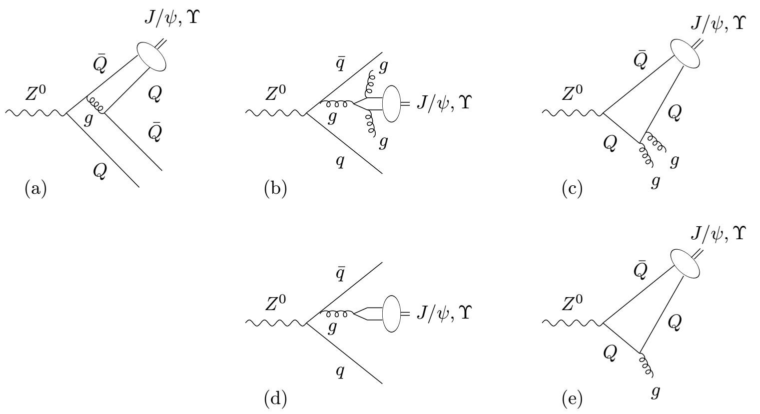

Fig. 1. Feynman diagrams for prompt heavy quarkonium production in Z^0 decays for (a) heavy quark fragmentation, (b,d) gluon fragmentation, (c,e) and hard gluon radiation, via color singlet (upper row) and color octet (lower row) quarkonium states.

tion process becomes dominant.[3] NRQCD calculations yield branching fractions of $B(Z^0 \to J/\psi ggX) = 1.9 \times 10^{-4}$ and $B(Z^0 \to \Upsilon ggX) = 4.1 \times 10^{-5}$.

We have searched for these processes in a sample of 3.25×10^6 produced hadronic Z^0 decays recorded in the DELPHI experiment. Our search included the J/ψ, ψ' and the three lowest Υ states, with decays to e^+e^- and $\mu^+\mu^-$.[4] The amount of charm-quark fragmentation into J/ψ was extracted from a fit to the inclusive J/ψ life time distribution.[5] Candidates were selected from hadronic Z^0 decays containing an isolated l^+l^- pair in the same hemisphere from the primary vertex (*i.e.* with decay lengths smaller than the vertex resolution) with lepton momenta above 3 GeV and a lepton energy sum above 10 GeV. Both leptons had to lie within 37^o of the jet axis, the missing energy of the event had to be less than 20% of the total energy, and any missing momentum had to be separated from the two leptons by more than 60^o. Candidates were separated into samples with a b-quark tag and a b-quark veto, by requiring that the probability for these tracks to originate from the primary vertex be $> 10\%$ or $< 10\%$, respectively. The quarkonium mass regions for $\mu^+\mu^-$ final states were defined as 2.96-3.24 GeV for the J/ψ, 3.51-3.85 GeV for the ψ', and 9.2-10.6 GeV for $\Upsilon(1S) - \Upsilon(3S)$ states. They were increased for e^+e^- final states to 2.6-3.86 GeV for J/ψ-ψ' states and 7.9-10.8 GeV for $\Upsilon(1S) - \Upsilon(3S)$ states to compensate for decay radiation and detector resolution effects.[†]

The efficiencies and background estimates for each mode have been determined from high statistics Monte Carlo samples for signal channels and generic hadronic Z^0 decays, respectively. The effect of b-quark tagging and decay vertex selection for signal and background modes was studied with events generated for direct $c \to$

[†]More details of the event selection are given in references 4 and 5.

$J/\psi X$ decays and for $b \to J/\psi X$ decays. We achieved efficiencies of $69 \pm 5\%$ and $59 \pm 12\%$ for the signal mode in the $\mu^+\mu^-$ and e^+e^- final states, while the $b \to J/\psi X$ background was reduced to $8.2 \pm 0.7\%$ and $9.5 \pm 0.9\%$, respectively. Furthermore, we have checked the inclusive dilepton invariant mass spectra for $b \to J/\psi X$ decays in the data and Monte Carlo. The two distributions show approximate agreement in the J/ψ mass region.

Potential backgrounds come from a) two subsequent semileptonic decays of a heavy quark, e.g. $b \to cl^-\bar{\nu} \to sl^+l^-\nu\bar{\nu}$, b) a heavy quark semileptonic decay plus a hadron misidentified as a lepton, c) $B \to J/\psi X$ and d) 4-Fermi processes such as $e^+e^- \to l^+l^-q\bar{q}$. The first two sources are suppressed by topology and vertex requirements. The residual backgrounds in the J/ψ and ψ' modes consists to 1/3 of $b \to J/\psi X$ events and to 2/3 of 4-Fermi events. The residual background in the Υ modes comes entirely from 4-Fermi processes.

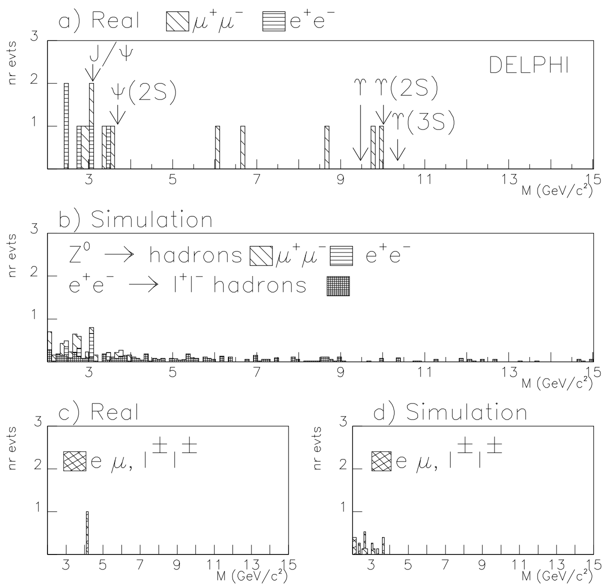

Fig. 2. Dilepton invariant mass spectra for a) data, b) simulated backgrounds of hadronic Z^0 decays and 4-Fermi processes and c-d) like sign dileptons plus $e^\pm\mu^\mp$ events in data and the Monte Carlo.

Figure 2 displays the l^+l^- invariant mass spectrum of our final candidates with a b-quark veto in the entire 2-15 GeV mass region. For comparison, the corresponding mass spectra of the simulated backgrounds and of studies of like-sign dileptons and $e^\pm\mu^\mp$ events are also shown. We observe 4 J/ψ candidates, 2 ψ' candidates and 2 Υ candidates. The individual event yields found in $\mu^+\mu^-$ and e^+e^- final states are summarized in Table I together with their detection efficiencies and background

Table 1. Results on prompt heavy quarkonia production

Channel $Z^0 \to$	$\epsilon(\mu\mu)[\%]$	$\epsilon(ee)$ [%]	background	$\mu\mu$ - ee yields	BR $\times 10^4$@90%CL
$c\bar{c} \to J/\psi c\bar{c}$	36.1 ± 0.5	13.6 ± 0.8	22.8 ± 4.7	$(6.0^{+5.0}_{-4.5})$	$>$ 4.3
$q\bar{q}g^* \to J/\psi ggX$	4.1 ± 0.5	2.5 ± 0.3	1.2 ± 0.4	2 (0) - 2 (0)	$>$ 4.1
ggJ/ψ	28 ± 2	17 ± 2			$>$ 0.61
$q\bar{q}g^* \to \psi' ggX$	0.2 ± 0.2	< 0.75	0.96 ± 0.31	1 (0) - 1 (0)	$>$ 20
$gg\psi'$	4.1 ± 0.5	2.5 ± 0.3			$>$ 2.7
$bb \to \Upsilon bb$	2.8 ± 1.0	1.7 ± 0.6	0.12 ± 0.04	2 (0) - 0 (0)	$>$ 6.1
$gg\Upsilon$	29 ± 3	11 ± 3	0.47 ± 0.14		$>$ 1.2
$q\bar{q}$ continuum			4.8 ± 1.5	5 (3) - 2 (1)	-

For each channel, efficiencies, backgrounds (combined for e^+e^- and $\mu^+\mu^-$ modes), event yields, and upper limits @ 90% CL for the branching ratios $B(Z^0 \to (Q\bar{Q})X)$ are listed. Event yields in the first (second) column show those for the b-quark veto (b-quark tag) selection.

estimates. These yields are higher than the residual background, but the excess observed is not significant. Thus, we set 90% CL branching ratio upper limits on heavy quarkonium production in Z^0 decays, using the observed yields, efficiencies, estimated backgrounds and systematic uncertainties (see Table I). The total systematic uncertainty amounts to 30%, with contributions from track reconstruction (12%), lepton identification (10%), isolated leptons (20%), vertex reconstruction (10%) and Monte Carlo statistics (12%).

For c-quark fragmentation into J/ψ and b-quark fragmentation into Υ states we obtain $B(Z^0 \to J/\psi c\bar{c}) < 4.3 \times 10^{-4}$ and $B(Z^0 \to \Upsilon b\bar{b}) < 6.1 \times 10^{-4}$ @ 90% CL, respectively.[6] These upper limits lie factors of 5.6 and 38 above the corresponding color singlet model NRQCD predictions. The upper limit for gluon fragmentation into J/ψ of $B(Z^0 \to J/\psi ggX) < 4.1 \times 10^{-4}$ @ 90% CL is just a factor of 2.2 above the color octet model NRQCD prediction. Our results are consistent with recent observations of prompt J/ψ and Υ production in the OPAL experiment.[7]

2. Search for B_c mesons in Z^0 decays

The main mechanism for $B_c^{\pm}$ meson production in Z^0 decays is the b-quark fragmentation process shown in figure 1a, where a hard gluon emitted from one of the b-quarks materializes into a $c\bar{c}$. This process is enhanced with respect to Υ production by $m_b^3/m_c^3 \simeq 40$.[8] W boson annihilation to $b\bar{c}$ is considerably reduced because of the small value of $\mid V_{cb} \mid^2$. The branching ratio predictions for $B_c^{\pm}$ production in Z^0 decays range from 1.2×10^{-4} to 5.7×10^{-4}, when contributions from the 2S, 3S, 1P and 2P states are included.[9] From potential models we obtain mass predictions of 6.25 ± 0.02 GeV for the $B_c^{\pm}$ ground state.[10]

The $B_c^{\pm}$ meson decay can proceed via b-quark decay, c-quark decay or via W boson annihilation, as shown in figure 3. This complex decay pattern influences the $B_c^{\pm}$ life time. The estimates range from 0.4 ps to 1.4 ps,[11] when an effective quark mass reduced by the binding energy is taken into account. In potential models, the branching ratios are predicted to be 37% for b-quark decay, 45% for c-quark decay and 18% for W boson annihilation.[9] For QCD sum rules the corresponding predictions yield 48%, 39%, and 13%, respectively.[12] Final states with a J/ψ are produced mainly through the color-allowed b-quark decay (Fig. 3a), yielding predictions of $B(B_c^{\pm} \to J/\psi X) = (10-24)\%$.[13]

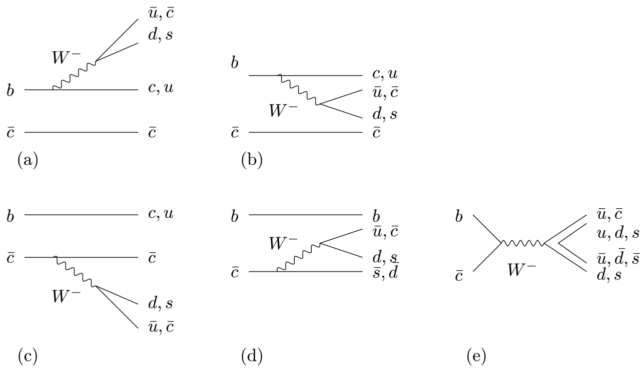

Fig. 3. Decays of $B_c^{\pm}$ mesons for a) color-allowed b-quark decay, b) color-suppressed b-quark decay, c) color-allowed c-quark decay d) color-suppressed c-quark decay, and e) W annihilation.

We have searched for $B_c^{\pm}$ mesons in 3.02×10^6 produced hadronic Z^0 decays accumulated in the DELPHI experiment. Our search focussed on four exclusive final states: $B_c^{\pm} \to J/\psi\pi^{\pm}$, $B_c^{\pm} \to J/\psi\pi^{+}\pi^{-}\pi^{\pm}$, $B_c^{\pm} \to J/\psi\mu^{\pm}\nu_{\mu}$, and $B_c^{\pm} \to J/\psi e^{\pm}\nu_e$, with J/ψ reconstruction in $\mu^+\mu^-$ and e^+e^-. The branching fractions are predicted to be $0.2-2\%$ for the hadronic modes and $1-5\%$ for the semileptonic modes.[14]

Our strategy consisted in selecting first an inclusive J/ψ sample from which exclusive final states were reconstructed by adding more particles, such as a $\pi^{\pm}$, $\pi^+\pi^-\pi^{\pm}$, a $\mu^{\pm}$, or an $e^{\pm}$. These extra particles were required to have momenta of $p > 0.2$ GeV, resolutions of $\sigma_p/p < 1$ and impact parameters of $\mathrm{d_t} < 2.5$ cm and $\mathrm{d_z} < 10.0$ cm for directions transverse and parallel to the beam. The inclusive sample consisted of 2420 events in the 2.5-3.5 GeV mass region with 2 oppositely charged leptons in the same hemisphere. The J/ψ reconstruction efficiency was only 37% due to stringent lepton identification criteria.

Since $B_c^{\pm}$ mesons originate from a secondary decay vertex, it is important to separate the B_c vertex from the primary vertex. We determined both vertices using an iterative fitting procedure. For 75% of the data we could perform only a 2-dimensional vertex fit in the $r-\phi$ plane, while for the remaining 25% we used a 3-dimensional vertex fit. For the fit to the primary vertex all charged tracks except for the l^+l^- pair were initially considered. Tracks with high χ^2 contributions were removed in the next iteration. If the probability of the new fit was less than 0.1%, the track with the largest χ^2 contribution was removed and the fit was repeated. This process was terminated, when the probability of the fit exceeded 0.1%. If only one track remained, the event was discarded. A similar procedure was then used to determine the $B_c^{\pm}$ decay vertex. The dilepton crossing point was used as a starting value. All charged tracks consistent with originating from this vertex were initially considered. As before, tracks with large χ^2 contributions were removed and the procedure terminated when the probability of the fit exceeded 0.1%.

If the angle between the separation vector $\vec{s}$ of the primary to secondary vertex and the J/ψ momentum vector was larger than 90^o, the event was rejected. In addition, $\mid \vec{s} \mid$ had to be larger than twice its error. The dilepton momentum was required to be above 2 GeV and the dilepton invariant mass had to satisfy $\mid m_{\mu\mu} - m_{J/\psi} \mid< 0.1$ GeV for dimuons and $-0.3 < m_{ee} - m_{J/\psi} < 0.1$ GeV for dielectrons. 277 events passed this selection yielding a 16% efficiency and a 77% purity. To reconstruct the four exclusive $B_c^{\pm}$ final states, only events with a J/ψ plus a $\pi^{\pm}$, $\pi^+\pi^-\pi^{\pm}$ or a charged lepton were considered, requiring that their impact parameters to the secondary vertex were less than 1 mm and less than 3 times the impact parameter resolution. The particle identification of the extra particles had to agree with expected particle hypothesis. In hadronic modes we defined $B_c^{\pm}$ signal regions of $6.0-6.5$ GeV for $\mu^+\mu^-(3)\pi$ and $5.8-6.7$ GeV for $e^+e^-(3)\pi$ final states, respectively. In semileptonic modes we considered every $J/\psi l^{\pm}$ mass combination above 4.0 GeV as $B_c^{\pm}$ signal. To remove spurious combinations of a J/ψ with extra particles we required that the angle $\Delta\phi$ between the momentum vector of the $J/\psi\pi$, $J/\psi l$ or $J/\psi 3\pi$ system and the vertex separation vector $\vec{s}$ be less than 10^o.‡

Table 2. Results for B_c meson searches in four exclusive final states with a J/ψ

Final state $B_c^{\pm} \to J/\psi X$	Yield	Background	ϵ[%] for 0.4 ps	ϵ[%] for 1.4 ps	BR $\times 10^5$ for 0.4 ps	limit @90%CL for 1.4 ps
$e^+e^-\pi^{\pm}$	0	1.1	3.1 ± 0.6	3.9 ± 0.5	$>$ 10	$>$ 8.4
$\mu^+\mu^-\pi^{\pm}$	1	0.6	9.0 ± 1.0	11.2 ± 1.0		
$e^+e^-3\pi^{\pm}$	0	0.9	1.9 ± 0.9	1.9 ± 0.9	$>$ 17	$>$ 17
$\mu^+\mu^-3\pi^{\pm}$	1	1.4	5.3 ± 1.0	5.3 ± 1.0		
$e^+e^-e^{\pm}\nu_e$	0	-	1.7 ± 0.4	2.3 ± 0.4	$>$ 16	$>$ 13
$\mu^+\mu^-e^{\pm}\nu_e$	0	-	3.9 ± 0.6	4.9 ± 0.7		
$e^+e^-\mu^{\pm}\nu_{\mu}$	0	-	3.3 ± 0.5	3.3 ± 0.5	$>$ 9.8	$>$ 9.1
$\mu^+\mu^-\mu^{\pm}\nu_{\mu}$	0	-	6.4 ± 0.8	7.5 ± 0.8		

The product branching ratio upper limits are for the ee and $\mu\mu$ modes combined

For efficiency determination and background studies, high statistic Monte Carlo samples for generic hadronic Z^0 decays and signal channels were generated. The data selection was studied for life times of 0.4 ps and 1.4 ps. Backgrounds originate from two semileptonic heavy quark cascade decays, and from color-suppressed B_u and B_d decays with a J/ψ in the final state. The first source is suppressed by our vertex requirements. The second source has the same topology as that of the signal modes. To remove this background, we performed an exclusive reconstruction of $B_{u,d} \to J/\psi K^{\pm,0} + (n\pi^0)$ decays with $n = 0, 2, 4$ π^0's and $B_{u,d} \to J/\psi K^{0,\pm} + (n\pi^{\pm})$ decays with $n = 1, 3, 5$ $\pi^{\pm}$'s. The charged kaons and pions were required to be associated with the secondary vertex and had to be identified correctly with the assigned particle hypothesis. Neutral particles were required to be in the same

‡Further details of the event selection are described reference 15.

hemisphere as the J/ψ. If the invariant mass of any such combination was within 100 MeV of the B_u and B_d mass, the candidate was removed from the final sample.

Figure 4 shows the $J/\psi\pi$ invariant mass spectra for candidates in the $J/\psi\pi^\pm$ final state for the data, background Monte Carlo and signal Monte Carlo before the $\Delta\phi$ requirement and before removing candidates consistent with a B_u or a B_d decay. Of the two candidates observed in figures 4a,b, the one in the $ee\pi$ final state is consistent with a $B^0 \to J/\psi K^+\pi^-$ decay, and thus removed from the final sample. In the semileptonic modes no candidate passes all the selection criteria, while in the $J/\psi 3\pi$ final state one candidate survives. The final yields are listed in Table II together with their efficiencies and background estimates. Since the observed yields in all four channels are consistent with the residual background, we present upper limits for the product branching ratios $B(Z^0 \to B_c^\pm X') \times B(B_c^\pm \to J/\psi X)$ @ 90 % CL for lifetimes of 0.4 ps and 1.4 ps (see Table II).

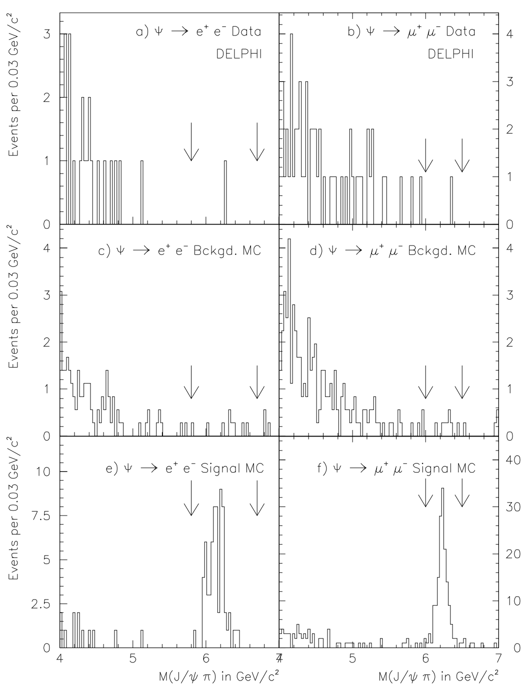

Fig. 4. $J/\psi\pi^\pm$ invariant mass distributions for (a & b) data, (c & d) simulated background normalized to the number of hadronic events in the data, and (e & f) signal Monte Carlo sample, for $e^+e^-\pi^\pm$ and $\mu^+\mu^-\pi^\pm$ final states, respectively. The arrows indicate the $B_c^\pm$ signal region.

The lowest product branching ratio upper limits are found for the $B_c^\pm \to J/\psi\pi^\pm$ and $B_c^\pm \to J/\psi\mu^\pm\nu_\mu$ decays which have the highest detection efficiencies. The upper limit on $B_c^\pm$ production can be lowered by combining the two semileptonic modes, where no candidates were found. The resulting upper limits are $B(Z^0 \to$

$B_c^{\pm}X) \times B(B_c^{\pm} \to J/\psi l^{\pm}\nu_l) < 5.8 \times 10^{-5}$ and $< 5.0 \times 10^{-5}$ @ 90% CL for life times of 0.4 and 1.4 ps, respectively [6] This is still a factor of 1.8 above the most optimistic prediction. Our upper limits are consistent with the results from the other LEP experiments.[16]

3. Evidence for radially excited B mesons

Hadronic $Z^0 \to b\bar{b}$ decays provide a rich source for producing excited B states. Using inclusive reconstruction methods, the transitions of $B^* \to B\gamma$, $B^{**} \to B\pi$, $B_{s1} \to BK$, $B_{s2} \to BK^*$, and $\Sigma_b^* \to \Lambda_b\pi$ have been clearly established.[17–19] We have also learned that $75\pm4\%$ of all B-mesons produced in Z^0 decays originate from B^*'s and that $29 \pm 4\%$ come from transitions of orbitally excited B states.[20] We have extended our inclusive analysis to $\pi^+\pi^-$ transitions to look for more excited B states. The data sample consisted of 3×10^6 Z^0 decays recorded with the DELPHI detector. Using the standard DELPHI b-quark tagging algorithm, we first obtained a b-quark enriched sample of 4×10^5 $b\bar{b}$ events.[21] This selection had an efficiency of $52\pm3\%$ and a purity of $80\pm4\%$. The inclusive reconstruction was based on a rapidity algorithm used in previous inclusive analyses[17]. Charged and neutral particles were configured into jets by a cluster algorithm. The rapidity η of each charged particle (assuming a π) and each neutral shower (assuming a γ) was then determined with respect to the jet axis. Only particles with $\eta > 1.5$ were considered as B-meson decay products. For these B-meson candidates a direction and an energy was determined. The energy determination was refined by applying a correction which depended both on the mass of the B candidate and the total energy reconstructed in the hemisphere containing the B-candidate.[17] Thus, an energy resolution of 7% was achieved for 75% of all B-mesons. The angular resolutions were 15 mr for 60% of the data and 38 mr for the remaining 40%.[§]

The inclusive B-meson candidates were then combined with a $\pi^+\pi^-$ pair originating from the primary vertex. To suppress the enormous combinatorial background, we selected only the $\pi^+\pi^-$ combination with the highest rapidity in the hemisphere of the B-candidate having $\eta > 2.5$. Performing vertex fits in a similar fashion as described in the previous section, we required that the probability of a fit to the primary vertex be greater than 2% while the probability of a fit to the B-decay vertex was less than 0.01%. For these candidates we determined the $Q = m(B^{(*)}\pi^+\pi^-) - m(B^{(*)}) - 2m(\pi^{\pm})$ value spectrum, shown in figure 5. Two narrow structures are apparent, which are fitted to two Gaussians plus a background shape obtained from Monte Carlo (solid curve). One narrow peak appears at $Q = 301 \pm 4 \pm 10$ MeV, has a width of $\sigma = 12 \pm 3$ MeV and shows an excess of 56 ± 13 events. The second narrow peak is observed at $Q = 220 \pm 4 \pm 10$ MeV, has a width of $\sigma = 15 \pm 3$ MeV and has a yield of 60 ± 12 events. The widths of these structures are compatible with the detector resolution, implying that their natural widths must be narrow.

[§] Further details are given in ref. 22

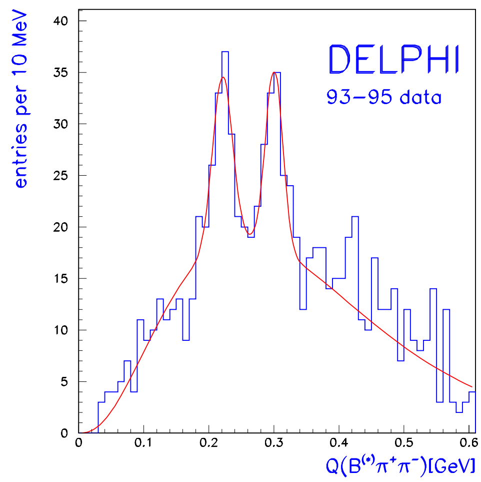

Fig. 5. The $Q = M(B^{(*)}\pi^+\pi^-) - M(B^{(*)} - 2M(\pi)$ spectrum. The solid line shows a fit to two Gaussians plus a background shape determined from the Monte Carlo.

To interpret these peaks it is useful to inspect the B-meson level diagram and the allowed hadronic transitions (see Fig. 6). Below 6 GeV four L=1 (1P) orbitally excited states and two radially excited (2S) states exist besides the 1S ground states. In heavy quark effective theory (HQET), the quantum numbers used to classify B states are the orbital angular momentum (l) and the total spin of the b-quark ($j = l \oplus 1/2$).[23] This leads to groups containing two states with similar properties. The two radially excited 2S states, denoted by B' and $B^{*\prime}$, are narrow. The orbitally excited states split up into two broad states with total spin $j = 1/2$, the $B_0^*(j = 1/2)$ and $B_1(j = 1/2)$, and two narrow states with total spin $j = 3/2$, the $B_1(j = 3/2)$ and $B_2^*(j = 3/2)$. Thus, the broad $j = 1/2$ states can be excluded from producing narrow peaks in figure 5. The allowed non-suppressed π and $\pi\pi$ transitions of the narrow $j = 3/2$ states are predicted to be: $B_1 \to B^*\pi$ via D-wave, and $B_1 \to B\pi\pi$ & $B_1 \to B^*\pi\pi$ via P-wave as well as $B_2^* \to B\pi$ & $B_2^* \to B^*\pi$ via D-wave, and $B_2^* \to B^*\pi\pi$ via P-wave. The corresponding decays of the radially excited states are: $B' \to B^*\pi$ via P-wave, and $B' \to B_0^*(j = 1/2)\pi$ & $B' \to B\pi\pi$ via S-wave, as well as $B^{*\prime} \to B\pi$ & $B^{*\prime} \to B^*\pi$ via P-wave, and $B^{*\prime} \to B_1(j = 1/2)\pi$ & $B^{*\prime} \to B^*\pi\pi$ via S-wave. ρ transitions are suppressed by phase space. Because of our good mass resolution we can exclude that a single excited state decays both to $B\pi\pi$ and $B^*\pi\pi$. If this were the case, we should observe two peaks in the Q-value spectrum separated by the hyperfine splitting of 46 MeV. This is definitely not observed. The Q-value spectrum, however, does not rule out that two excited states, separated by ~ 46 MeV, decay (the heavier state to $B^*\pi\pi$ and the lighter state to $B\pi\pi$).

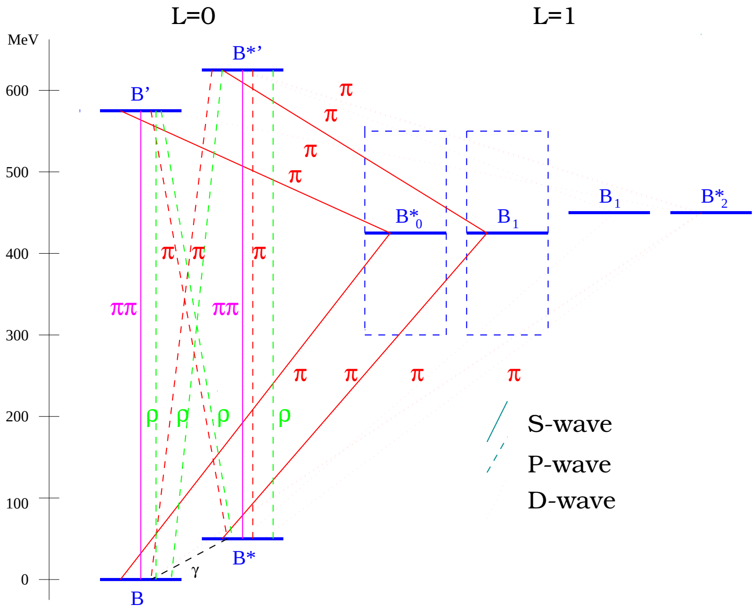

Fig. 6. B-meson level diagram with hadronic transitions predicted in the quark model.

The lower peak is consistent with $\pi\pi$ transitions from the $B_1(j = 3/2)$ and $B_2^*(j = 3/2)$ orbital excitations, as a similar structure is observed in the Q-value spectrum for $B^{(*)}\ \pi$ transitions. So, we observe most likely the P-wave transitions, $B_1 \to B\pi^+\pi^-$ with possible contributions from $B_2^* \to \pi^+\pi^- B^*$. The upper peak has to originate from states which lie $\geq$ 80 MeV above the narrow $B_1(j = 3/2)$ orbital excitation. Considering the remaining possibilities, the most likely interpretation is that the upper peak stems from transitions $B' \to B\pi\pi$ and $B^{*\prime} \to B^*\pi\pi$ of the 2S radial excitations. We expect the main contribution to come from the S-wave $\pi\pi$ transitions, similar to those observed in the Υ system, eg. $\Upsilon' \to \pi\pi\Upsilon$. To determine the amount of two successive π transitions via the broad 1P states, which are kinematically forbidden in the Υ system, requires more detailed studies. Single π transitions $B' \to B\pi$ are also allowed. But they are expected to be suppressed due to nodes in the radial wave functions, which lead to cancellations in the overlap integral.[24] Nevertheless, the observed Q-value spectrum of the $B^{(*)}\pi$ transitions actually has room for such transitions. Our interpretation is supported by predictions from QCD based relativistic quark models, as the observed Q-values are consistent with those predicted.[25] Our observation places the masses of the radial excitations to $M(B') = 5860$ MeV and $M(B^{*\prime}) = 5905$ MeV with uncertainties of the order of 12 MeV. From the yields we can determine a preliminary estimate of the production cross sections, yielding $\sigma(b \to B' + B^{*\prime})/\sigma(b) = 0.5\% - 4\%$. The branching ratio for $B_1 \to B\pi\pi$ is of the order of $2\% - 10\%$.

Acknowledgements

I would like to thank all members of the DELPHI collaboration, especially M. Feindt, G.P. Gopal, R. Keränen, and C. Kreuter for their support and useful discussions.

References

1. E. Braaten *et al.*, *Phys. Rev. D48* (1993) 4230; V. Barger *et al.*, *Phys. Rev. D41* (1990) 1541.
2. W.Y. Keung *Phys. Rev. D23* (1981) 2072; K. Hagiwara *et al.*, *Phys. Lett B267* (1991) 527, with erratum in *Phys. Lett. B316* (1993) 631; E. Braaten and T.C. Yuan, *Phys. Lett. 71* (1993) 1673, and *Phys. rev. D50* (1994) 3176.
3. P. Cho *Phys. Lett. B368* (1996) 171; P. Cho and A. Leibovich, *Phys. Rev. D53* (1996) 150.
4. P. Abreu *et al.*, Z. Phys. C69 (1996) 575;
5. P. Abreu *et al.*, *Phys. Lett. B341* (1994) 109.
6. Use $B(Z^0 \to q\bar{q}) = 69.9 \pm 0.15\%$ from R.M. Barnett *et al.* (Particle Data Group), *Phys. Rev. D54* (1996) 1.
7. G. Alexander *et al.*, *Phys. Lett. B341* (1996) 185; G. Alexander *et al.*, *Phys. Lett. B384* (1996) 343.
8. E. Braaten, Y.Q. Chen and T.C. Yuan, *Phys. Rev. D48* (1993) 5049.
9. E. Braaten, Y.Q. Chen and T.C. Yuan, *Phys. Rev. D48* (1993) 5049, V.V Kiselev, A.K. Likhoded, and M.V. Shevlyagin, *Phys. Atom. Nucl. 57* (1994) 689; T.C. Yuan, *Phys. Rev. D50* (1994), 5664; Y.Q. Chen *Phys. Rev. D48* (1993) 5181.
10. W. Kwong and J.L. Rosner, *Phys. Rev. D44* (1991) 212; E. Eichten and C. Quigg, *Phys. Rev. D49* (1994) 5845; E. Bagan, *et al.*, *ISN-93-123* (1994).
11. C. Quigg *FERMILAB-Conf-93/265-T*; C.H. Chang and Y.Q. Chen, *Phys. Rev. D49* (1994) 3399; M. Lusignoli and M.Masetti, *Z. Phys. C51* (1991) 549.
12. D. London *UdeM-LPN-TH-93-178* (1993).
13. M. Lusignoli and M.Masetti, *Z. Phys. C51* (1991) 549; A. Leike and R. Rückl, *Nucl. Phys. Proc. Suppl. 37B* (1994) 215; V.V. Kiselev *IHEP 95-80, hep-ph/9507228* (1995).
14. M. Lusignoli and M.Masetti, *Z. Phys. C51* (1991) 549 D. London *UdeM-LPN-TH-93-178* (1993); A. Leike and R. Rückl, *Nucl. Phys. Proc. Suppl. 37B* (1994) 215.
15. M.L. Andrieux *et al.*, *ICHEP'96 DELPHI 96-CONF-25* (1996).
16. M. McNeil *see these procceedings*; ALEPH collaboration, *ICHEP Conference*, Warsaw (1996) PA01-069; G. Alexander *et al.*, *Z. Phys. C70* (1996) 197; L3 Collaboration, *ICHEP Conference* Warsaw (1996) PA05-046.
17. M. Acciarri *et al.*, *Phys. Lett. B345* (1995) 589; P. Abreu *et al.*, *Z. Phys C68* (1995) 353; D. Busculic *et al.*, *Z. Phys. C69* (1996) 393.
18. R. Akers *et al.*, *Z. Phys. C66* (1995) 19; P. Abreu *et al.*, *Phys. Lett. B345* (1995) 598.
19. M Feindt *et al.*, DELPHI-95-105 (1995).
20. M. Feindt, *CERN-PPE/95-139*, *Proc. Hadron '95*, World Scientific (1995) 84.
21. D. Buskulic *et al.*, *Phys. Lett. B313* (1993) 535; P. Abreu *et al.*, *CERN-PPE-/94-131* (1994).
22. M. Feindt and O. Podobrin, *ICHEP'96 DELPHI 96-CONF-22* (1996).
23. E.J. Eichten, C.T. Hill and C. Quigg, *Phys. Rev. Lett. 71* (1993) 4116.
24. R. Kokoski and N. Isgur, *Phys. Rev. D35* (1987) 907.
25. S. Godfrey and N. Isgur, *Phys. Rev. D32* (1985) 189.